

Dimers of Boroglycine and Methylamine Boronic Acid: A Computational Comparison of the Relative Importance of Dative *versus* Hydrogen Bonding

Joseph D. Larkin,^{†,‡} Matt Milkevitch,[§] Krishna L. Bhat,^{||} George D. Markham,[⊥] Bernard R. Brooks,[‡] and Charles W. Bock^{*,§,⊥}

Department of Chemistry, Bloomsburg University of Pennsylvania, Bloomsburg, Pennsylvania 17815, Department of Chemistry and Biochemistry, School of Science and Health, Philadelphia University, School House Lane and Henry Avenue, Philadelphia, Pennsylvania 19144, The Institute for Cancer Research, Fox Chase Cancer Center, 7701 Burholme Avenue, Philadelphia, Pennsylvania 19111, National Heart, Lung, and Blood Institute, The National Institutes of Health, Building 50, Bethesda, Maryland 20851, and Department of Chemistry, Widener University, Chester, Pennsylvania 19011

Received: August 14, 2007; In Final Form: September 24, 2007

Boronic acids are widely used in materials science, pharmacology, and the synthesis of biologically active compounds. In this Article, geometrical structures and relative energies of dimers of boroglycine, $\text{H}_2\text{N}-\text{CH}_2-\text{B}(\text{OH})_2$, and its constitutional isomer $\text{H}_3\text{C}-\text{NH}-\text{B}(\text{OH})_2$, were computed using second-order Møller–Plesset perturbation theory and density functional theory; Dunning–Woon correlation-consistent cc-pVDZ, aug-cc-pVDZ, cc-pVTZ, and aug-cc-pVTZ basis sets were employed for the MP2 calculations, and the Pople 6-311++G(d,p) basis set was employed for a majority of the DFT calculations. Effects of an aqueous environment were incorporated into the results using PCM and COSMO-RS methodology. The lowest-energy conformer of the $\text{H}_2\text{N}-\text{CH}_2-\text{B}(\text{OH})_2$ dimer was a six-membered ring structure (chair conformation; C_i symmetry) with two intermolecular B:N dative-bonds; it was 14.0 kcal/mol *lower* in energy at the MP2/aug-cc-pVDZ computational level than a conformer with the classic eight-centered ring structure (C_i symmetry) in which the boroglycine monomers are linked by a pair of $\text{H}-\text{O}\cdots\text{H}$ bonds. Compared to the results of MP2 calculations with correlation-consistent basis sets, DFT calculations using the PBE1PBE and TPSS functionals with the 6-311++G(d,p) basis set were significantly better at predicting relative conformational energies of the $\text{H}_2\text{N}-\text{CH}_2-\text{B}(\text{OH})_2$ and $\text{H}_3\text{C}-\text{NH}-\text{B}(\text{OH})_2$ dimers than corresponding calculations using the BLYP, B3LYP, OLYP, and O3LYP functionals, particularly with respect to dative-bonded structures.

Introduction

Organoboronic acids ($\text{R}-\text{B}(\text{OH})_2$) and boronate esters ($\text{R}-\text{B}(\text{OR}')_2$) have found remarkable utility as reagents for carbon–carbon bond formation^{1–3} and are widely used for the synthesis of pharmaceutical agents.^{4–6} Interest in organoboronic acids also arises from their potent biological activity,⁷ *e.g.*, boronic–amino acid derivatives are strong inhibitors of human arginase II, whose primary function appears to be in L-arginine and nitric oxide homeostasis.⁸ Related α -amino boronic acid derivatives are well-known for their ability to act as inhibitors of serine proteases and β -lactamases.^{3,9–11} Organoboronic acids also serve as chemical sensors for 1,2- and 1,3-diols,^{12–20} as affinity ligands in chromatographic protocols,^{21–25} as therapeutic agents in boron neutron capture therapy (BNCT) for the treatment of certain brain tumors,²⁶ as antibiotics,²⁷ and as building blocks in the development of novel materials^{28–32} and supramolecular assemblies.³³

Despite the increasing number of applications of boronic acids,² many aspects of their geometrical structures, reactivity, and thermochemistry are not well understood.³⁴ A survey of

crystal structures in the Cambridge Structural Database (CSD)^{35,36} containing the $\text{C}-\text{B}(\text{OH})_2$ moiety showed that organoboronic acids often form eight-centered, doubly hydrogen-bonded ring dimers in the solid state; see Scheme 1.^{37–44} Indeed, the asymmetric unit in the X-ray crystal structure of phenylboronic acid (PBA) consisted of two molecules of the acid linked by a pair of $\text{H}-\text{O}\cdots\text{H}$ bonds;⁴⁵ the hydroxyl hydrogen atoms of each monomer were in the *exo-endo* arrangement shown in Scheme 1.

The hydrogen-bonding pattern in Scheme 1, in which the boron atoms have nearly planar, trigonal coordination, has also been observed in crystal structures of other arylboronic acids,^{30–33,35,38} and it is similar to that found in dimers formed from the $-\text{CONH}_2$ and $-\text{COOH}$ functional groups,^{46–48} where resonance assisted hydrogen bonding (RAHB) is an important factor.^{49,50} Other hydrogen-bonding patterns⁵¹ have also been observed with organoboronic acids, *e.g.*, the crystal structure of 5-pyrimidylboronic acid involving (B)O–H \cdots N hydrogen bonds with ring nitrogen atoms;⁵² the motif shown in Scheme 1 was not evident.⁴¹

In a computational investigation of the hydrolysis of diborane, B_2H_6 , McKee⁵³ reported that the lowest-energy conformer of the $\text{HB}(\text{OH})_2$ dimer, was a planar, doubly hydrogen-bonded structure with C_{2h} symmetry, in which the hydroxyl groups of both monomers were in the *exo-endo* orientation; see Scheme 1 ($\text{R} = \text{H}$). Recently, using second-order Møller–Plesset perturbation theory (MP2),⁵⁴ coupled-cluster calculations,^{55–58}

* Corresponding author. Telephone: (570) 389-4154. E-mail: jllarkin@bloomu.edu.

[†] Bloomsburg University of Pennsylvania.

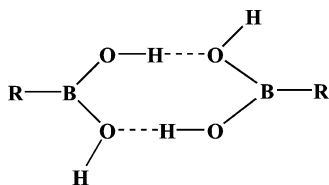
[‡] The National Institutes of Health.

[§] Philadelphia University.

^{||} Widener University.

[⊥] Fox Chase Cancer Center.

SCHEME 1



and a variety of density functional theory (DFT) methods with Pople split-valence^{59,60} and Dunning–Woon correlation-consistent (cc) basis sets,^{61–64} we confirmed that the McKee structure was the lowest-energy conformer of the boronic acid dimer;⁶⁵ its dimerization energy, enthalpy, and free energy were computed to be -10.8 , -9.2 , and $+1.2$ kcal/mol, respectively, at the MP2(FC)/aug-cc-pVTZ level. A variety of other singly and doubly hydrogen-bonded, OH-bridged, and H-bridged dimeric structures were also identified as stationary points on the PES, although they were all higher in energy than the C_{2h} structure.

In the present study, geometrical structures and relative energies of the neutral, achiral, α -amino boronic acid $H_2N-CH_2-B(OH)_2$ (boroglycine) dimer were investigated using MP2/cc methodology. Several derivatives of this acid, including some isoelectronic and isostructural analogs, have shown promise as chymotrypsin inhibitors^{66,67} and, more recently, the peptide L- γ -Gly-L-Leu-(aminomethyl)boronic acid, have been shown to be a stronger inhibitor of glutathionyl spermidine synthetase than the phosphonic acid analog, making it an attractive target for the design of antiparasitic drugs.⁶⁸ From a computational perspective, dimers of this simple α -amino boronic acid provide an opportunity to study the relative importance of intermolecular B:N and B:O dative (coordination) bonds as compared to O-H \cdots O and O-H \cdots N hydrogen bonds. Because it is well-established that compounds of the form $H_2N-CHR-B(OH)_2$ can undergo a 1,2-carbon-to-nitrogen rearrangement to give the isomer $H_2RC-NH-B(OH)_2$,^{2,69} we also investigated dimers of methylamine boronic acid, $H_3C-NH-B(OH)_2$. To the authors' knowledge, no previous experimental or computational studies of α -amino boronic acid dimers have been reported in the literature. Recently, however, Rogowska *et al.*⁷⁰ presented structural evidence for strong heterodimeric interactions between phenylboronic acid (PBA) and L-proline and betaine in the solid state,^{71–73} and they supported their conclusions with computational results; in particular, they reported a dimerization energy for the zwitterion $(H_3C)_3N^+CH_2COO^-$ with PBA of -25.5 kcal/mol *in vacuo* at the MP2/6-31+G(d) level.

Although derivatives of boroglycine have intriguing chemical properties,^{66–68} most α -amino organoboronic acids of importance are substantially larger and calculations using MP2 methodology with large cc basis sets are not yet practical; DFT calculations with Pople-type basis sets are an attractive alternative, but the reliability of specific functional/basis-set combinations for describing boronic acid chemistry has yet to be established. Unfortunately, there are indications that the popular BLYP and B3LYP, as well as the newer OLYP and O3LYP functionals, have problems predicting the strength of B:N and/or B:O dative bonds.^{65,74–79} To address this DFT reliability issue for the dimerization of α -amino boronic acids, our MP2 results using cc basis sets were compared to those obtained with the BLYP, B3LYP, OLYP, O3LYP, PBE1PBE, and TPSS functionals using the 6-311++G(d,p) basis set; in selected cases comparisons were also made with the B3LYP and PBE1PBE functionals using cc basis sets.

Computational Methods

Equilibrium geometries in this article were obtained using MP2⁵⁴ with the frozen core (FC) option; Dunning–Woon, correlation-consistent cc-pVDZ, cc-pCVDZ, aug-cc-pVDZ, cc-pVTZ, and aug-cc-pVTZ basis sets were employed.^{61–64} Whenever our computational resources permitted, frequency analyses were performed analytically or numerically, depending on the computational efficiency, to confirm that the optimized structures were local minima on the PES and to correct dimerization enthalpies and free energies to 298K. Dimer stabilization energies (SE) were computed using the supermolecule approach, $SE = E_{dimer} - \sum E_{monomers}$, and corrected for basis set superposition errors (BSSEs) using the counterpoise procedure. Calculations were performed using GAUSSIAN 03.⁸⁰ Atomic charges were obtained from natural population analyses (NPA); wavefunctions were analyzed with the aid of natural bond orbitals.^{81–85}

DFT geometry optimizations were performed with the following functionals: BLYP and B3LYP, which incorporate the dynamical functional of Lee, Yang, and Parr (LYP),⁸⁶ coupled with Becke's pure DFT exchange functional (B);⁸⁷ OLYP⁸⁸ and O3LYP,⁸⁹ constructed from the novel OPTX exchange functional; PBE1PBE,^{90,91} which makes use of the one-parameter generalized-gradient approximation (GGA) PBE functional⁹² with a 25% exchange and 75% correlation weighting; and TPSS, the nonempirical meta-generalized gradient approximation (MGGA) functional recently developed by Staroverov, Scuseria, Tao, and Perdew.⁹³ The economical Pople 6-311++G(d,p)^{59,60} basis set was used for most of the DFT calculations, although in selected cases comparisons were made with results from a variety of cc basis sets.

Self-consistent reaction field (SCRF) calculations in aqueous media were carried out with the IEF polarizable continuum model (PCM);^{94–98} such continuum methods have well-known limitations in describing protic solvents.^{99,100} Calculations using a conductor-like screening model (COSMO)^{101–104} were performed using the PQS *Ab Initio* Program Package 3.2;¹⁰⁵ we employed the default settings in the COSMO module in this software package were tailored for COSMO-RS theory^{106,107} using the BPV86 functional, *i.e.*, the BP86 functional^{108,109} with local correlation replaced by VWN¹¹⁰ with the tzvp-Ahlich's basis set.^{111,112}

Results and Discussion

$H_2N-CH_2-B(OH)_2$ and $H_3C-NH-B(OH)_2$ Monomers. There are no experimental geometrical structures of $H_2N-CH_2-B(OH)_2$ monomers available in the literature. Indeed, this simple α -amino boronic acid has been observed only as a TFA or HCl salt in acidic media.^{113,114} However, computed geometry-optimized structures and relative energies of a variety of its conformers were reported recently at quite high computational levels.¹¹⁵ In the lowest-energy form of this monomer the N–C–B–O backbone was nonplanar, the hydroxyl groups were in the *exo-endo* orientation, and the structure was stabilized to some extent by an *intramolecular* O–H \cdots N hydrogen bond. A number of other *exo-endo* conformers, as well as a conformer in which the hydroxyl groups were in an *anti* orientation, were less than 5 kcal/mol higher in energy, whereas conformers in which the hydroxyl groups were in a *syn* arrangement were more than 5 kcal/mol higher in energy.

Computational studies also showed that the hydroxyl groups of the lowest-energy form of the $H_3C-NH-B(OH)_2$ monomer were in the *exo-endo* orientation, although the C–N–B–O backbone in this geometrical structure was planar.¹¹⁵ In general,

conformers of $\text{H}_3\text{C}-\text{NH}-\text{B}(\text{OH})_2$ were significantly lower in energy than the corresponding conformers of $\text{H}_2\text{N}-\text{CH}_2-\text{B}(\text{OH})_2$.¹¹⁵

$\text{H}_2\text{N}-\text{CH}_2-\text{B}(\text{OH})_2$ Dimers. A variety of intermolecular hydrogen-bonding and dative-bonding interactions between two $\text{H}_2\text{N}-\text{CH}_2-\text{B}(\text{OH})_2$ monomers are possible. An extensive conformational search of the $\text{H}_2\text{N}-\text{CH}_2-\text{B}(\text{OH})_2$ dimer potential energy surface (PES) was initially performed at the economical PBE1PBE/6-311++G(d,p) computational level. Our experience utilizing the PBE1PBE functional with the 6-311++G(d,p) basis set for boronic acid derivatives has been positive; it provides reasonable geometries and relative energies compared to those from the more rigorous MP2/aug-cc-pVDZ computational level;^{65,74,115–117} nevertheless, some caution must be exercised in interpreting results at the PBE1PBE/6-311++G(d,p) level (*vide infra*). Numerous stationary points on the $\text{H}_2\text{N}-\text{CH}_2-\text{B}(\text{OH})_2$ dimer PES were identified at this DFT level; the resulting conformers were subsequently re-optimized at various MP2 computational levels.

Figure 1A shows structures of the lowest-energy local minima that we found for several distinct classes of $\text{H}_2\text{N}-\text{CH}_2-\text{B}(\text{OH})_2$ dimers; relative energies are listed in Table 1A, and dimerization energies are given in Table 2A. Cartesian coordinates of selected $\text{H}_2\text{N}-\text{CH}_2-\text{B}(\text{OH})_2$ dimers at several MP2 computational levels are given in Table 1S of the Supporting Information.

Although the hydrogen-bonded structural motif shown in Scheme 1 was the global minimum on the $\text{H}-\text{B}(\text{OH})_2$ dimer PES *in vacuo* and in the SCRF-PCM representation of aqueous media,^{53,65} and it is the most fundamental structural motif found for boronic acids in the solid state,^{35,36,70} preliminary PBE1PBE/6-311++G(d,p) results strongly indicated that it was *not* the global minimum on the $\text{H}_2\text{N}-\text{CH}_2-\text{B}(\text{OH})_2$ dimer PES. Nevertheless, we decided to employ the lowest-energy form of the boroglycine dimer with this motif, **1** (C_i) in Figure 1A, as a baseline from which to compare relative energies of all the dimers in this investigation. The geometrical structure of the nearly planar eight-centered ring in **1** was similar to that of the corresponding boronic acid dimer,⁶⁵ although the length of the $\text{O}-\text{H}\cdots\text{O}$ hydrogen bond was ~ 0.04 Å shorter at the same computational levels, indicative of stronger hydrogen bonding.¹¹⁸ Indeed, the calculated dimerization enthalpy of $\text{H}_2\text{N}-\text{CH}_2-\text{B}(\text{OH})_2$ was -11.3 kcal/mol at the MP2/aug-cc-pVDZ computational level (see Table 2A), compared to -9.2 kcal/mol for $\text{H}-\text{B}(\text{OH})_2$. Numerous other local minima in which $\text{H}_2\text{N}-\text{CH}_2-\text{B}(\text{OH})_2$ monomers were linked by a pair of $\text{O}-\text{H}\cdots\text{O}$ hydrogen bonds and the boron atom coordination was (nearly) trigonal planar were also located—the hydroxyl groups in these dimers were in a variety of forms (*exo-endo*, *syn*, or *anti*)—but they were all ~ 10 kcal/mol or more higher in energy than **1** at a variety of computational methods.

Several doubly (H)O-bridged conformers of the $\text{H}_2\text{N}-\text{CH}_2-\text{B}(\text{OH})_2$ dimer, in which both boron atoms are tetracoordinated, were also optimized. The lowest-energy form we found, **2** (C_s) in Figure 1A, was 14.4 kcal/mol higher in energy than **1** at the MP2/aug-cc-pVDZ level (Table 1A); the corresponding bridged dimer of $\text{H}-\text{B}(\text{OH})_2$ was 12.8 kcal/mol above the minimum-energy C_{2h} form at this level.¹¹⁵ The two distinct bridging B–O distances in **2** are similar in value, 1.58 and 1.61 Å at the MP2/aug-cc-pVDZ level; the B–O single bond lengths in the $\text{H}_2\text{N}-\text{CH}_2-\text{B}(\text{OH})_2$ monomer at this level are ~ 1.38 Å, in good agreement with typical experimental values,⁴⁵ and the O:B dative bond length in the simple heterodimer $\text{H}_2\text{O}:\text{BH}_3$ is ~ 1.77 Å.¹¹⁹ In addition, the composition of the four boron–oxygen ring bonding orbitals in **2** are all quite similar, indicating considerable

redistribution of electron density upon dimer formation (HOMOs of **2** and the corresponding monomer are plotted in Figure 1S of the Supporting Information). This stabilizing electronic contribution, however, is counteracted by steric issues associated with the structure of the compact four-centered ring in **2**, which distorts the tetrahedral bonding around the boron atoms, *e.g.*, the O–B–O angles in the ring are only $\sim 89^\circ$. Furthermore, there is significant electrostatic repulsion in this conformer between the two highly charged boron atoms ($q_B = \sim +1.05e$) which are in quite close proximity, as are the two ring oxygen atoms ($q_O = \sim -0.84e$).

Dimers of $\text{H}_2\text{N}-\text{CH}_2-\text{B}(\text{OH})_2$ linked by one or two $\text{O}-\text{H}\cdots\text{N}$ hydrogen bonds were also investigated (see conformers **3** (C_1) and **4** (C_2), respectively in Figure 1A); in structure **3** the monomers were also bound together by an $\text{O}-\text{H}\cdots\text{O}$ hydrogen bond. Although the boron atoms have (nearly) planar trigonal coordination in both conformers, the structure of the nine- and ten-centered hydrogen-bonded rings in **3** and **4** were highly nonplanar. These conformers were found to be 1.2 and 3.5 kcal/mol lower in energy than the eight-membered doubly $\text{O}-\text{H}\cdots\text{O}$ hydrogen-bonded ring conformer **1** at the MP2/aug-cc-pVDZ level (Table 1A) and, after correction for BSSE the dimerization energies of **1**, **3**, and **4**, were all quite similar; see Table 2A.

Although the role of intramolecular B:N dative bonding in the $\text{H}_2\text{N}-\text{CH}_2-\text{B}(\text{OH})_2$ monomer has yet to be established,¹¹⁵ intermolecular B:N dative bonding in the corresponding dimer proved to be extremely important, *e.g.*, conformers **5a** (C_1) and **5b** (C_1) involved one tetracoordinated boron atom with a short boron–nitrogen distance, ~ 1.66 Å at the MP2/aug-cc-pVDZ level, and results from NPA analyses were consistent with the presence of a B:N dative bond; the geometry surrounding the other boron atom in each of these conformers was (nearly) trigonal planar. For comparison, we note that the calculated boron–nitrogen distance in the simple heterodimer $\text{H}_3\text{N}:\text{BH}_3$, ~ 1.67 Å,¹¹⁹ is nearly the same at this computational level. (Experimental boron–nitrogen dative-bonded distances range from ~ 1.57 Å in cubic boron nitride¹²⁰ to ~ 2.91 Å, the sum of the van der Waals radii of boron and nitrogen.¹²¹) The calculated values of the Höpfl index for **5a** and **5b**, a measure of the tetrahedral character of the boron atom in these derivatives, are quite high, 75.8% and 66.5% at the MP2/aug-cc-pVDZ level,¹²² and both **5a** and **5b** are slightly lower in energy than **1**, *e.g.*, by 3.2 and 6.9 kcal/mol, respectively, at the MP2/aug-cc-pVDZ level; conformers **5a** and **5b** are also bound by $\text{O}-\text{H}\cdots\text{O}$ and $\text{O}-\text{H}\cdots\text{N}$ hydrogen bonds, respectively, in seven-centered ring structures (Figure 1A) and, similar to what we observed for dimer structures **3** and **4**, the lower-energy conformer, **5b**, is involved the $\text{O}-\text{H}\cdots\text{N}$ hydrogen bond.

The global minimum on the $\text{H}_2\text{N}-\text{CH}_2-\text{B}(\text{OH})_2$ dimer PES was the doubly B:N dative-bonded, six-membered ring, chair conformer, **6** (C_i) (Figure 1A), at all the MP2 computational levels we employed in this study; the corresponding boat conformer was ~ 3 kcal/mol higher in energy at a variety of levels. Both hydroxyl groups in **6** were in the *exo-endo* orientation. The calculated boron–nitrogen bond distances in **6** were ~ 1.65 Å at the MP2/aug-cc-pVDZ level, approximately 0.02 Å shorter than that found in **5a**, **5b**, and $\text{H}_3\text{N}:\text{BH}_3$; the Höpfl index for each of the boron atoms in **6** was quite high, 73.1%.¹²² The computed dimerization enthalpy of **6**, -25.1 kcal/mol at the MP2/aug-cc-pVDZ level, is extremely high (Table 2); the resulting value after correction for BSSE is much less negative, -12.7 kcal/mol.

In summary, conformer **6** (with two B:N dative bonds) was 7.1 kcal/mol lower in energy than **5b** (with one N:B dative bond

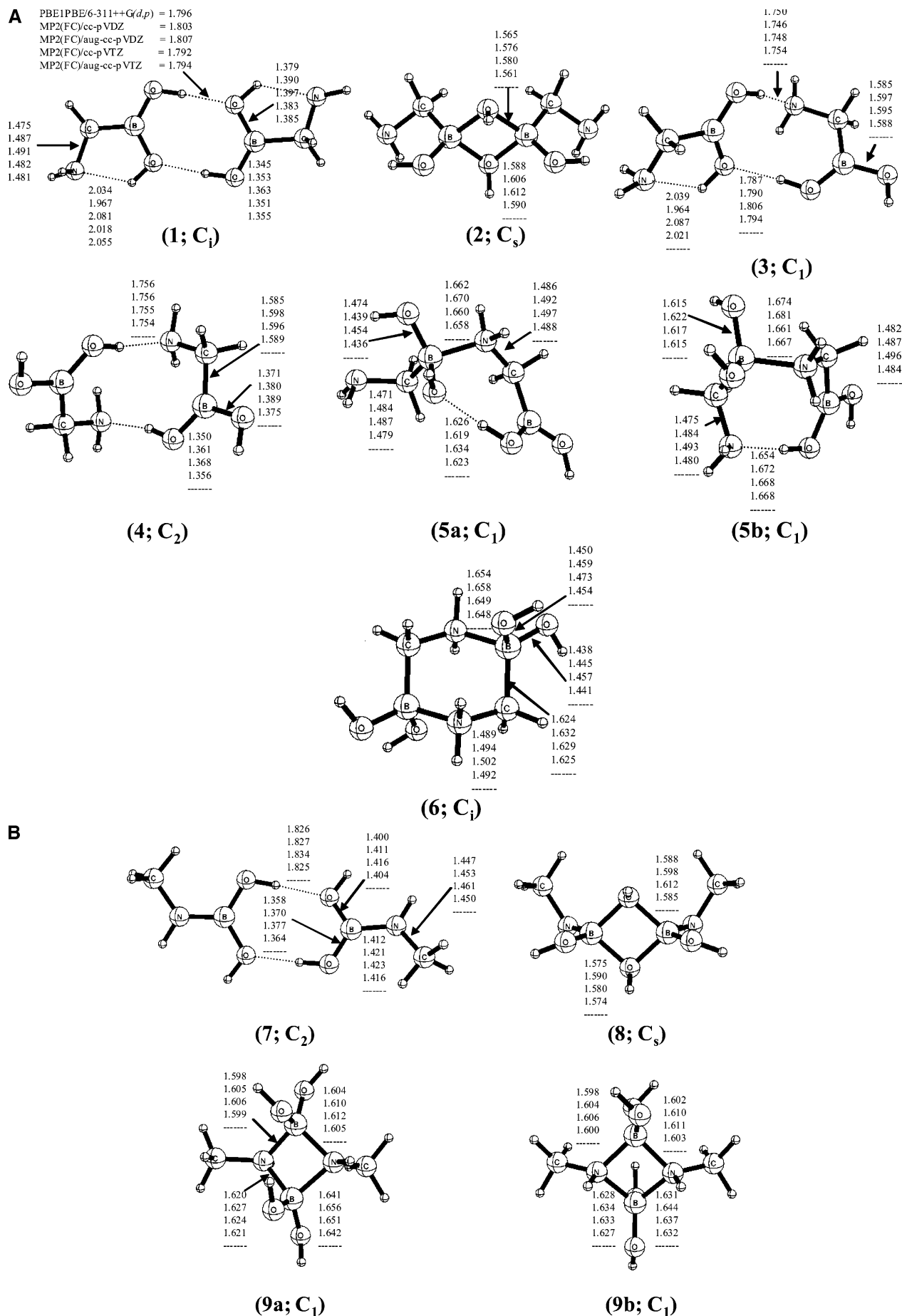


Figure 1. Optimized structures of (A) $H_2N-CH_2-B(OH)_2$ and (B) $H_3C-NH-B(OH)_2$ dimers. Distances are in Å, and angles are in deg.

TABLE 1: Relative Energies, E (kcal/mol) (Values Thermally Corrected to 298 K in Parentheses), for Various Conformers of the (A) $\text{H}_2\text{N}-\text{CH}_2-\text{B}(\text{OH})_2$ and (B) $\text{H}_3\text{C}-\text{NH}-\text{B}(\text{OH})_2$ Dimers at the (DFT) PBE1PBE/6-311++G(d,p) Computational Level and Several MP2(FC) Levels with Correlation-Consistent Basis Sets

(A) $\text{H}_2\text{N}-\text{CH}_2-\text{B}(\text{OH})_2$ Dimers							
level	dimer						
	1	2	3	4	5a	5b	6
PBE1PBE/6-311++G(d,p)	0.0 (0.0)	+20.6 (+19.9)	-0.1 (-0.2)	-0.4 (-0.7)	+3.0 (+3.2)	+0.1 (-0.04)	-3.8 (-3.6)
MP2(FC)/cc-pVDZ	0.0 (0.0)	+17.9 (+17.0)	-1.3 (-1.4)	-3.1 (-3.2)	+0.1 (+0.2)	-3.2 (-3.5)	-8.0 (-8.0)
MP2(FC)/aug-cc-pVDZ	0.0 (0.0)	+14.4 (+13.5)	-1.2 (-1.4)	-3.5 (-3.7)	-3.2 (-3.1)	-6.9 (-7.1)	-14.0 (-13.8)
MP2(FC)/cc-pVTZ	0.0	+16.2	-1.0	-2.9	-0.8	-4.6	-10.5
MP2(FC)/aug-cc-pVTZ	0.0						

(B) $\text{H}_3\text{C}-\text{NH}-\text{B}(\text{OH})_2$ Dimer				
level	dimer			
	7	8	9a	9b
PBE1PBE/6-311++G(d,p)	-34.2(-34.7)	-2.5(-4.1)	-27.0(-27.7)	-27.2(-27.8)
MP2(FC)/cc-pVDZ	-34.3(-34.6)	-8.3(-9.8)	-35.3(-35.9)	-35.5(-36.1)
MP2(FC)/aug-cc-pVDZ	-34.9(-35.0)	-9.5(-10.7)	-37.1(-37.6)	-36.8(-37.3)
MP2(FC)/cc-pVTZ	-37.0	-10.3	-36.7	-36.7
MP2(FC)/aug-cc-pVTZ	-37.1			

TABLE 2: Dimerization Energies, E (kcal/mol) (Values Corrected for BSSE in Parentheses), for Various Dimers of (A) $\text{H}_2\text{N}-\text{CH}_2-\text{B}(\text{OH})_2$ and (B) $\text{H}_3\text{C}-\text{NH}-\text{B}(\text{OH})_2$ at the (DFT) PBE1PBE/6-311++G(d,p) Computational Level and Several MP2(FC) Levels with Correlation Consistent Basis Sets

(A) $\text{H}_2\text{N}-\text{CH}_2-\text{B}(\text{OH})_2$ Dimers ^a						
conf		PBE1PBE/ 6-311++G(d,p)	MP2(FC)/			
			cc-pVDZ	aug-cc-pVDZ	cc-pVTZ	aug-cc-pVTZ
1	ΔE	-12.1 (-11.3)	-14.4 (-9.4)	-12.9 (-10.3)	-12.8 (-10.8)	-12.9
	ΔH^0_{298}	-10.5	-12.8	-11.3		
	ΔG^0_{298}	-0.1	-2.8	-1.1		
3	ΔE	-12.2 (-10.9)	-15.7 (-7.1)	-14.2 (-10.5)	-13.8 (-10.3)	
	ΔH^0_{298}	-10.7	-14.2	-12.7		
	ΔG^0_{298}	-0.2	-3.3	-2.0		
4	ΔE	-12.5 (-10.9)	-17.5 (-6.3)	-16.4 (-11.4)	-15.7 (-10.8)	
	ΔH^0_{298}	-11.2	-16.1	-15.1		
	ΔG^0_{298}	-0.1	-4.8	-3.2		
5a	ΔE	-9.1 (-6.9)	-14.3 (-5.8)	-16.1	-13.6	
	ΔH^0_{298}	-7.3	-12.7	-14.4		
	ΔG^0_{298}	+5.7	+0.4	-1.2		
5b	ΔE	-12.0 (-9.4)	-17.6 (-8.3)	-19.9 (-10.8)	-17.3	
	ΔH^0_{298}	-10.6	-16.3	-18.5		
	ΔG^0_{298}	+2.4	-3.5	-5.0		
6	ΔE	-15.9 (-13.4)	-22.4 (-12.2)	-26.9 (-14.5)	-23.4	
	ΔH^0_{298}	-14.1	-20.9	-25.1		
	ΔG^0_{298}	-0.2	-7.1	-10.9		

(B) $\text{H}_3\text{C}-\text{NH}-\text{B}(\text{OH})_2$ Dimers ^b						
conf		PBE1PBE/ 6-311++G(d,p)	MP2(FC)/			
			cc-pVDZ	aug-cc-pVDZ	cc-pVTZ	aug-cc-pVTZ
7	ΔE	-10.7 (-9.8)	-13.1 (-7.3)	-11.5 (-9.0)	-11.3 (-9.1)	-11.4
	ΔH^0_{298}	-9.1	-11.5	-9.9		
	ΔG^0_{298}	+0.6	-1.5	-0.3		
9a	ΔE	-3.5 (-0.2)	-14.1(-3.6)	-13.7	-11.1	
	ΔH^0_{298}	-2.1	-12.8	-12.4		
	ΔG^0_{298}	+13.0	+2.7	+3.2		
9b	ΔE	-3.6 (-0.3)	-14.4(-3.6)	-13.5	-11.0	
	ΔH^0_{298}	-2.2	-13.0	-12.2		
	ΔG^0_{298}	+12.9	+2.1	+2.9		

^a In all cases the monomers were taken as the lowest-energy conformer of $\text{H}_2\text{N}-\text{CH}_2-\text{B}(\text{OH})_2$.¹¹⁵ ^b In all cases the monomers were taken as the lowest-energy conformer of $\text{H}_3\text{C}-\text{NH}-\text{B}(\text{OH})_2$.¹¹⁵

and one $\text{O}-\text{H}\cdots\text{N}$ hydrogen bond), 10.5 kcal/mol *lower* in energy than **4** (with two $\text{O}-\text{H}\cdots\text{N}$ hydrogen bonds), 10.8 kcal/mol *lower* in energy than **5a** (with one N:B dative bond and one $\text{O}-\text{H}\cdots\text{N}$ hydrogen bond), 12.8 kcal/mol *lower* in energy than **3** (with one $\text{O}-\text{H}\cdots\text{O}$ hydrogen bond and one $\text{O}-\text{H}\cdots\text{N}$ hydrogen bond), and 14.0 kcal/mol *lower* in energy than **1** (with

two $\text{O}-\text{H}\cdots\text{O}$ hydrogen bonds) at the MP2/aug-cc-pVDZ level. These findings clearly emphasize the important role of *intermolecular* B:N dative bonds and $\text{O}-\text{H}\cdots\text{N}$ hydrogen bonds in boroglycine dimers in the gas phase; *intermolecular* B:O dative and $\text{O}-\text{H}\cdots\text{O}$ hydrogen bonds appear to play a lesser role in these dimers.

H₃C–NH–B(OH)₂ Dimers. As noted previously, compounds of the form H₂N–CHR–B(OH)₂ can undergo a 1,2-carbon-to-nitrogen (Matteson) rearrangement to give the constitutional isomer H₂RC–NH–B(OH)₂.² Thus, we also investigated dimers of methylamine boronic acid, H₃C–NH–B(OH)₂. Structures of the lowest-energy local minima that we found for several distinct classes of H₃C–NH–B(OH)₂ dimers are shown in Figure 1B, relative energies are listed in Table 1B, and dimerization energies are given in Table 2B. It is important to emphasize that the energies of these methylamine boronic acid dimers are significantly *lower* than their boroglycine analogs, in accord with the corresponding results for the monomers.¹¹⁵

The lowest-energy conformer, **7** (C₂), of the H₃C–NH–B(OH)₂ dimer that was found in the initial PBE1PBE/6-311++G(d,p) exploration of the PES had the classic, eight-centered, doubly O–H···O hydrogen-bonded ring structure; at the MP2/aug-cc-pVDZ computational level **7** was 34.9 *lower* in energy than the corresponding conformer **1** of the H₂N–CH₂–B(OH)₂ dimer and 20.9 kcal/mol *lower* in energy than the doubly dative-bonded conformer **6**; see Table 1B. The length of the O–H···O hydrogen bonds in **7**, however, were actually ~0.25 Å *longer* than in **1**, and this structural feature was reflected in the corresponding dimerization enthalpies; *e.g.*, the value of ΔH₂₉₈⁰ for **7** was –9.9 kcal/mol at the MP2/aug-cc-pVDZ level compared to –11.3 kcal/mol for **1**. Thus, the large energy separation between the homologous dimers **1** and **7** is predominantly a result of the large energy difference between the corresponding monomers¹¹⁵ rather than a result of stronger hydrogen bonding. Several other local minima on the H₃C–NH–B(OH)₂ dimer PES with two O–H···O hydrogen bonds or with one O–H···O hydrogen bond and one O–H···N hydrogen bond were also located, but these conformers were higher in energy than **7** at a variety of computational levels. Contrary to what we observed for conformer **1**, some geometrical details of the computed structure of dimer **7** were quite sensitive to the inclusion of diffuse functions; *i.e.*, at the MP2/aug-cc-pVDZ level, the eight-centered ring in **7** was nearly planar, whereas at the MP2/cc-pVDZ and MP2/cc-pVTZ levels, it was significantly nonplanar.

The structure of the four-centered (–B–O–B–O–) ring in the (H)O-bridged conformer **8** (C_s) of the H₃C–NH–B(OH)₂ dimer was similar to that in the analogous conformer **2** of the H₂N–CH₂–B(OH)₂ dimer (Figure 1B), as was the composition of the NPA ring B–O bonding orbitals. Interestingly, however, **8** was only 23.9 kcal/mol *lower* in energy than **2**, whereas **7** was 34.9 kcal/mol *lower* in energy than **1** at the MP2/aug-cc-pVDZ level. The additional destabilization of **8** was in part caused by an increase in electrostatic repulsion between the boron atoms which were found to be ~0.1e *more* positive in **8** than in **2**. It should be mentioned, however, that conformer **8** is still lower in energy than any of the H₂N–CH₂–B(OH)₂ dimer conformers we located, except the doubly B:N dative-bonded conformer **6**; see Table 1.

The doubly nitrogen-bridged structures **9a** (C₁) and **9b** (C₁) shown in Figure 1B, were ~7 kcal/mol *higher* in energy than conformer **7** at the PBE1PBE/6-311++G(d,p) level we employed in the initial survey of the H₃C–NH–B(OH)₂ dimer PES, but these novel geometrical structures proved to be ~2 kcal/mol *lower* in energy than **7** at the MP2/aug-cc-pVDZ level (Table 1B) and appear to be the global minima on the H₃C–NH–B(OH)₂ PES at this level. The boron–nitrogen distances in the four-centered rings in **9a** and **9b** vary from ~1.61 to ~1.65 Å at the MP2/aug-cc-pVDZ level and are as much as 0.04 Å shorter than the corresponding distance in the six-

centered ring in the dative-bonded conformer **6**. For comparison, the B–N single-bond distances in conformer **7** were ~1.42 Å at the MP2/aug-cc-pVDZ level and the B:N dative bond distance in H₃N:BH₃ was 1.67 Å. Thus, despite significant steric issues, *e.g.*, the N–B–N bond angle in the ring is ~90° at this level, and substantial electrostatic repulsion between the two boron atoms (+1.15e) and between the two nitrogen atoms (–0.86e) in the ring, these structures are the lowest-energy forms we found on the H₃C–NH–B(OH)₂ dimer PES.

PCM and COSMO-RS Calculations in Aqueous Media. Keeping in mind that PCM-SCRF calculations in protic media have some well-established limitations,^{99,100} we re-optimized the gas-phase conformers **1–6** of the H₂N–CH₂–B(OH)₂ dimers and **7–9** of the H₃C–NH–B(OH)₂ dimers using the IEF-PCM SCRF representation of aqueous media at the PBE1PBE/6-311++G(d,p) level.¹²³ The dative-bonded conformer **6** in this simple model was lower in energy than conformers **1–5**, similar to what we observed *in vacuo*, although the energy separations were often accentuated, *e.g.*, **6** was 6.3 kcal/mol lower in energy than **4** in aqueous media, compared to only 3.4 kcal/mol in the gas phase. The homologous, doubly hydrogen-bonded form of the H₃C–NH–B(OH)₂ dimer, **7**, was 25.8 kcal/mol lower in energy than **6** in (PCM) aqueous media compared to 30.4 kcal/mol *in vacuo*.

Concerns about the reliability of the PCM PBE1PBE/6-311++G(d,p) calculations in aqueous media¹²³ led us to consider COSMO-RS model calculations;^{106,107} such calculations tend to be more reliable for high-dielectric media such as water. The BPV86/tzvp-Ahlrichs computational level^{108,109,111,112} was employed using the PQS *Ab Initio* Program Package 3.2.¹⁰⁵ At this level the dative-bonded conformer **6** was predicted to be the lowest in energy of the H₂N–CH₂–B(OH)₂ dimers, 5.9 kcal/mol *lower* in energy than **1** (Table 2S); in the gas phase **6** was 2.1 kcal/mol *higher* in energy than **1** at this level, in accord with results from a variety of other DFT methods (*vide infra*), but in stark contrast to MP2 results; see Table 1. At this COSMO-RT computational level the lowest-energy form of the H₃C–NH–B(OH)₂ dimer was **7**, 35.3 kcal/mol lower in energy than **1** compared to only 32.7 kcal/mol *in vacuo*.

Thus, although predicted structural and relative energies of the H₂N–CH₂–B(OH)₂ and H₃C–NH–B(OH)₂ dimers in aqueous media depend to some extent on the computational model employed for the water continuum, it appears that the relative importance of B:N dative-bonded conformers is greater in solution than it is *in vacuo*.

DFT versus MP2 Comparison. In Table 3 we list relative energies of conformers **1–6** of the H₂N–CH₂–B(OH)₂ dimers and **7–10** of the H₃C–NH–B(OH)₂ dimers *in vacuo* using the TPSS, B3LYP, BLYP, O3LYP, OLYP, and PBE1PBE functionals with the Pople 6-311++G(d,p) basis set; the corresponding BVP86/tzvp-Ahlrichs energies are listed in Table 2S. In comparing these DFT results with the MP2 results in Table 1 there are certainly a number of encouraging points. For example, the large MP2 energy difference between the dimers H₂N–CH₂–B(OH)₂ (**1**) and H₃C–NH–B(OH)₂ (**7**), both of which have the classic eight-centered hydrogen-bonded ring structure, was quite well reproduced at all the DFT/6-311++G(d,p) levels. In addition, DFT/6-311++G(d,p) level relative energies of the O–H···O and O–H···N hydrogen-bonded dimers **1**, **3**, and **4**, are generally in good agreement with the corresponding MP2 results. The high MP2 energies of the (H)O-bridged dimers **2** and **8**, relative to the double hydrogen-bonded conformers **1** and **7**, respectively, were also predicted at all the DFT/6-311++G(d,p) levels, although the magnitude of the

TABLE 3: Relative Energies (kcal/mol) (Values Thermally Corrected to 298 K in Parentheses), for Various Dimers of (A) $\text{H}_2\text{N}-\text{CH}_2-\text{B}(\text{OH})_2$ and (B) $\text{H}_3\text{C}-\text{NH}-\text{B}(\text{OH})_2$ Using the TPSS, B3LYP, BLYP, O3LYP, OLYP, and PBE1PBE Functionals with the 6-311++G(d,p) Basis Set

(A) $\text{H}_2\text{N}-\text{CH}_2-\text{B}(\text{OH})_2$ Dimers							
functional	dimer						
	1	2	3	4	5a	5b	6
TPSSTPSS	0.0 (0.0)	+20.9 (+20.2)	-0.2 (-0.3)	-0.3 (-0.5)	+4.6 (+4.7)	+1.8 (+1.6)	-0.7 (-0.6)
B3LYP	0.0 (0.0)	+27.1 (+26.2)	-0.1 (-0.1)	-0.1 (-0.4)	+7.3 (+7.5)	+4.8 (+4.6)	+4.5 (+4.6)
BLYP	0.0 (0.0)	+29.6 (+28.7)	-0.2 (-0.3)	-0.4 (-0.7)	+9.1 (+9.2)	+6.5 (+6.2)	+8.6 (+8.7)
O3LYP	0.0 (0.0)	+25.6 (+24.9)	-0.1 (-0.2)	-0.1 (-0.3)	+8.0 (+8.3)	+5.8 (+5.7)	+5.2 (+5.5)
OLYP	0.0 (0.0)	+26.7 (+26.0)	-0.2 (-0.3)	-0.2 (-0.4)	+9.2 (+9.4)	+6.9 (+6.7)	+7.4 (+7.7)
PBE1PBE	0.0 (0.0)	+20.5 (+19.7)	-0.1 (-0.2)	-0.4 (-0.7)	+3.0 (+3.2)	+0.1 (-0.0 ₄)	-3.8 (-3.6)

(B) $\text{H}_3\text{C}-\text{NH}-\text{B}(\text{OH})_2$ Dimers				
functional	dimer			
	7	8	9a	9b
TPSSTPSS	-35.7 (-35.8)	-4.0 (-5.3)	-26.3 (-26.8)	-26.6 (-26.9)
B3LYP	-36.4 (-36.9)	+2.2 (+0.6)	-19.8 (-20.5)	-20.0 (-20.6)
BLYP	-34.9 (-35.1)	+5.5 (+4.1)	-15.1 (-15.8)	-15.3 (-15.9)
O3LYP	-34.8 (-35.3)	+2.1 (+0.6)	-19.7 (-20.3)	-20.1 (-20.6)
OLYP	-33.7 (-34.1)	+3.9 (+2.4)	-17.3 (-17.8)	-17.7 (-18.2)
PBE1PBE	-34.2 (-34.7)	-2.5 (-4.1)	-27.0 (-27.7)	-27.2 (-27.8)

energy separation was consistently overestimated, particularly using the BLYP, B3LYP, OLYP, and O3LYP functionals, suggesting that calculations at these levels underestimate the strength of boron–oxygen dative interactions. This remains true even with better basis sets, *e.g.*, at the B3LYP/cc-pVDZ, B3LYP/aug-cc-pVDZ, and B3LYP/cc-pVTZ levels, the energies of **2** are 25.2, 24.9, and 26.3 kcal/mol higher in energy than **1** (Table 2S), some 10 kcal/mol greater than that found at the corresponding MP2 levels (Table 1A), suggesting some deficiency with the B3LYP functional rather than the basis set.

The most serious problem with the DFT/6-311++G(d,p) calculations concerns the relative energies of conformers that involve B:N. For example, the BLYP, B3LYP, OLYP, and O3LYP functionals with the 6-311++G(d,p) basis set find conformer **6** to be 4–9 kcal/mol *higher* in energy than **1**, whereas MP2 calculations with several different correlation-consistent basis sets find **6** to be 8–14 kcal/mol *lower* in energy than **1**. To identify the origin of this discrepancy, we note that at the MP2/6-311++G(d,p) level, conformer **6** is 11.1 kcal/mol *lower* in energy than **1**, whereas at the B3LYP/cc-pVDZ, B3LYP/aug-cc-pVDZ, and B3LYP/cc-pVTZ levels **6** is 3.3, 1.9, and 4.8 kcal/mol, respectively, *higher* in energy than **1**. Thus, it appears that the BLYP, B3LYP, OLYP, and O3LYP functionals, independent of the basis set, seriously underestimate the strength of boron–nitrogen dative bonds compared to the corresponding MP2 results. It is important to note that the TPSS and PBE1PBE functionals with the 6-311++G(d,p) basis set perform much better in this regard, *e.g.*, **6** is predicted to be 0.7 and 3.8 kcal/mol, respectively, *lower* in energy than **1**; see Table 3. Furthermore, using the PBE1PBE functional with the cc-pVTZ basis set, conformer **6** is ~ 3 kcal/mol *lower* in energy than **1**.

We also calculated the energy difference between conformers **1** and **6** of the $\text{H}_2\text{N}-\text{CH}_2-\text{B}(\text{OH})_2$ dimers using the progression of pure SVWN5(LDA), PBE, and TPSS functionals to assess the effect of climbing “Jacob’s Ladder” in describing B:N dative bonds at this level.¹²⁴ The calculated energy differences were -9.0, -0.0₄, and -0.7 kcal/mol with the 6-311++G(d,p) basis set and -10.9, -2.1, and -2.7 kcal/mol with the aug-cc-pVDZ basis set. Although the SVWN5/6-311++G(d,p) energy results are in surprisingly good agreement with the corresponding MP2 calculations using correlation-consistent basis sets, calculated geometries at this level are not particularly good. The PBE and

TPSS results show significant improvement in the calculated geometries and the energy difference improves slightly in going from PBE to TPSS.

Concluding Remarks

Boronic acids are widely used in materials science and pharmacology, as well as in the synthesis of biologically active compounds. One of the drawbacks of using these acids, however, is the structural ambiguity associated with them, *e.g.*, under anhydrous conditions, boronic acids dimerize (and/or trimerize) to form anhydrides and boroxines.¹²⁵ In this Article, geometrical structures and relative energies of various conformers of $\text{H}_2\text{N}-\text{CH}_2-\text{B}(\text{OH})_2$ and $\text{H}_3\text{C}-\text{NH}-\text{B}(\text{OH})_2$ dimers were computed using MP2 methodology with correlation-consistent basis sets and using DFT with the economical 6-311++G(d,p) basis set.

The lowest-energy conformer of the $\text{H}_2\text{N}-\text{CH}_2-\text{B}(\text{OH})_2$ dimer using MP2 methodology with several correlation-consistent basis sets was the doubly dative-bonded six-membered ring structure, **6**, which was 14.0 kcal/mol *lower* in energy than the classic doubly H–O \cdots H hydrogen-bonded eight-centered ring structure, **1**, at the MP2/aug-cc-pVDZ computational level; furthermore, conformer **6** was 7.1 kcal/mol *lower* in energy than **5b** (one N:B bond; one O–H \cdots N bond), 10.5 kcal/mol *lower* in energy than **4** (two O–H \cdots N bonds), 10.8 kcal/mol *lower* in energy than **5a** (one N:B bond; one O–H \cdots N bond), and 12.8 kcal/mol *lower* in energy than **3** (one O–H \cdots O bond; one O–H \cdots N bond). These findings emphasize the role of *intermolecular* B:N dative and O–H \cdots N hydrogen bonding for boroglycine dimers in the gas phase. The dimerization enthalpy of the classic doubly H–O \cdots H hydrogen-bonded eight-centered ring structures of $\text{H}_2\text{N}-\text{CH}_2-\text{B}(\text{OH})_2$, -11.3 kcal/mol at the MP2/aug-cc-pVDZ computational level, was nearly 3 kcal/mol more negative than the corresponding value for H–B(OH)₂, -8.6 kcal/mol.

Compounds of the form $\text{H}_2\text{N}-\text{CHR}-\text{B}(\text{OH})_2$ can also undergo a 1,2-carbon-to-nitrogen rearrangement of the -B(OH)₂ moiety to give the isomeric structure $\text{H}_2\text{RC}-\text{NH}-\text{B}(\text{OH})_2$.^{2,69} Calculations at several MP2 and DFT levels clearly demonstrated that various $\text{H}_3\text{C}-\text{NH}-\text{B}(\text{OH})_2$ dimers were substan-

tially lower in energy than the corresponding $\text{H}_2\text{N}-\text{CH}_2-\text{B}(\text{OH})_2$ dimers, *e.g.*, the doubly hydrogen-bonded conformer, **7**, of $\text{H}_3\text{C}-\text{NH}-\text{B}(\text{OH})_2$ was ~ 35 kcal/mol lower in energy than the corresponding doubly hydrogen-bonded conformer, **1**, of $\text{H}_2\text{N}-\text{CH}_2-\text{B}(\text{OH})_2$. Interestingly, both of the novel doubly nitrogen-bridged structures, **9a** and **9b**, were slightly lower in energy than the doubly hydrogen-bonded structure **7**; see Table 1.

PCM (PBE1PBE/6-311++G(d,p)) and COSMO-RS (BPV86/tzvp-Ahlrichs) calculations in aqueous media predict that dative-bonded conformers are lower in energy than hydrogen-bonded conformers compared to the corresponding results *in vacuo*.

DFT/6-311++G(d,p) calculations do well in predicting the relative energies of $\text{O}-\text{H}\cdots\text{O}$ and $\text{O}-\text{H}\cdots\text{N}$ hydrogen-bonded dimers but underestimate the strength of boron-oxygen and boron-nitrogen dative interactions. For calculations on large α -amino boronic acids, where MP2 calculations with a large correlation-consistent basis set are not yet possible, the PBE1PBE functional with the Pople 6-311++G(d,p) basis set appears to be a viable alternative.

Acknowledgment. This research was supported in part by the Intramural Research Program of the NIH, NHLBI. K.L.B. thanks the National Textile Center (C03-PH01); G.D.M. thanks the NIH (GM31186, CA06927) and NCI for financial support of this work, which was also supported by an appropriation from the Commonwealth of Pennsylvania. The following Fox Chase Cancer Center Facilities were used in the preparation of this manuscript: the High Performance Computing Facility and the Research Secretarial Services.

Supporting Information Available: Table 1S containing Cartesian coordinates of selected $\text{H}_2\text{N}-\text{CH}_2-\text{B}(\text{OH})_2$ and $\text{H}_3\text{C}-\text{NH}-\text{B}(\text{OH})_2$ dimers at various MP2 computational levels. Table 2S containing relative COSMO-RS energies (kcal/mol) of (A) $\text{H}_2\text{N}-\text{CH}_2-\text{B}(\text{OH})_2$ and (B) $\text{H}_3\text{C}-\text{NH}-\text{B}(\text{OH})_2$ at the BVP86/tzvp-Ahlrichs computational level (corresponding gas-phase results are listed in parentheses). Figure of optimized geometries. This material is available free of charge via the Internet at <http://pubs.acs.org>.

References and Notes

- Chemler, S. R.; Trauner, D.; Danishefsky, S. J. *Angew. Chem., Int. Ed. Engl.* **2001**, *40*, 4544–4568.
- Hall, D. G. *Boronic Acids*, 1st ed.; Wiley-VCH Verlag: Berlin, 2005; p 545.
- Matteson, D. S. *Chem. Rev.* **1989**, *89*, 1535–1551.
- Yang, W.; Gao, X.; Wang, B. *Med. Res. Rev.* **2003**, *23* (3), 346–368.
- Miyaura, N.; Suzuki, A. *Chem. Rev.* **1995**, *95*, 2457–2483.
- Suzuki, A. *Metal-catalyzed cross-coupling reactions*; Wiley-VCH: Weinheim, Germany, 1998; Chapter 2.
- Blacquiere, J. M.; Sicora, O.; Vogels, C. M.; Cuperlovic-culf, M.; Decken, A.; Ouellette, R. J.; Westcott, S. A. *Can. J. Chem.* **2005**, *83*, 2052–2059.
- Cama, E.; Colleluori, D. M.; Emig, F. A.; Shin, H.; Kim, S. W.; Kim, N. N.; Traish, A. M.; Ash, D. E.; Christianson, D. W. *Biochemistry* **2003**, *42* (28), 8445–8451.
- Di Costanzo, L.; Sabio, G.; Mora, A.; Rodriguez, P. C.; Ochoa, A. C.; Centeno, F.; Christianson, D. W. *Proc. Natl. Acad. Sci. U.S.A.* **2005**, *102*, 13058–13063.
- Benini, S.; Rypniewski, W.; Wilson, K. S.; Mangani, S.; Ciurli, S. *J. Am. Chem. Soc.* **2004**, *126*, 3714–3715.
- Chen, Y.; Shoichet, B. K.; Bonnet, R. *J. Am. Chem. Soc.* **2005**, *127*, 5423–5434.
- Wang, W.; Gao, X.; Wang, B. *Curr. Org. Chem.* **2002**, *6*, 1285–1317.
- Ni, W.; Fang, G.; Springsteen, B.; Wang, B. *J. Org. Chem.* **2004**, *69*, 1999–2007.
- Franzen, S.; Ni, W.; Wang, B. *J. Phys. Chem. B* **2003**, *107*, 12942–12948.
- Steigler, S. *Curr. Org. Chem.* **2003**, *7*, 81–102.
- Philips, M. D.; James, T. D. *J. Fluores* **2004**, *14*, 549–559.
- Springsteen, G.; Wang, B. H. *Tetrahedron* **2002**, *58* (26), 5291–5300.
- Koumoto, K.; Takenchi, M.; Shinkai, S. *Supramol. Chem.* **1998**, *9*, 203.
- Otsuka, H.; Uchimura, E.; Koshino, H.; Okano, T.; Kataoka, K. *J. Am. Chem. Soc.* **2003**, *125* (12), 3493–3502.
- Cordes, D. B.; Gamsey, S.; Singaram, B. *Angew. Chem., Int. Ed.* **2006**, *45* (23), 3829–3832.
- Liu, X. C.; Scouten, W. H. *J. Chromatogr. A* **1994**, *687*, 61–69.
- Wulff, G. *Angew. Chem., Int. Ed. Engl.* **1995**, *34*, 1812–1832.
- Westmark, P. R.; Valencia, L. S.; Smith, B. D. *J. Chromatogr. A* **1994**, *664*, 123–128.
- Liu, G.; Hubbard, J. L.; Scouten, W. H. *J. Organomet. Chem.* **1995**, *493*, 91–94.
- Psotova, L. *Chem. Listy* **1995**, *89*, 641–648.
- Soloway, A. H.; Tjarks, W.; Barnum, B. A.; Rong, F. G.; Barth, R. F.; Codogni, I. M.; Wilson, J. G. *Chem. Rev.* **1998**, *98* (4), 1515–1562.
- Irving, A. M.; Vogels, C. M.; Nikolcheva, L. G.; Edwards, J. P.; He, X. F.; Hamilton, M. G.; Baerlocher, M. O.; Baerlocher, F. J.; Decken, A.; Westcott, S. A. *New J. Chem.* **2003**, *27*, 1419–1424.
- Abrahams, B. F.; Haywood, M. G.; Robson, R. *J. Am. Chem. Soc.* **2005**, *127* (3), 816–817.
- Li, Y.; Ruoff, R. S.; Chang, R. P. H. *Chem. Mater.* **2003**, *15*, 3276–3285.
- Parry, P. R.; Wang, C.; Batsanov, A. S.; Bryce, M. R.; Tarbit, B. *J. Org. Chem.* **2002**, *67*, 7541–7543.
- Wang, W.; Zhang, Y.; Huang, K. *J. Phys. Chem. B* **2005**, *109*, 8562–8564.
- Wang, W. J.; Zhang, Y.; Huang, K. *Chem. Phys. Lett.* **2005**, *405*, 425–428.
- Pedireddi, V. R.; SeethaLekshmi, N. *Tetrahedron Lett.* **2004**, *45*, 1903–1906.
- Yan, J.; Springsteen, G.; Deeter, S.; Wang, B. H. *Tetrahedron* **2004**, *60*, 11045–11205.
- Allen, F. H. *Acta Crystallogr. B* **2002**, *58*, 380–388.
- Allen, F. H.; Kennard, O. *Chem. Design Automation News* **1993**, *8*, 31–37.
- Aakeröy, C. B.; Salmon, D. J. *CrystEngComm* **2005**, *7*, 439–448.
- Bradley, D. C.; Harding, I. S.; Keefe, A. D.; Motevalli, M.; Zhen, D. H. *J. Am. Chem. Soc.* **1996**, *118*, 3931–3936.
- Fournier, J. H.; Maris, T.; Wuest, J. D.; Guo, W.; Galoppini, E. *J. Am. Chem. Soc.* **2003**, *125*, 1002–1006.
- Gainsford, G. J.; Meinhold, R. H.; Woolhouse, A. D. *Acta Crystallogr. C* **1995**, *51*, 2694–2696.
- Maly, K. E.; Maris, T.; Wuest, J. D. *CrystEngComm* **2006**, *8*, 33–35.
- Rodriguez-Cuamatzi, P.; Vargas-Diaz, G.; Höpfl, H. *Angew. Chem., Int. Ed.* **2004**, *43*, 3041–3044.
- Zarychta, B.; Zaleski, J.; Sporzynski, A.; Dabrowski, M.; Serwatowski, J. *Acta Crystallogr. C* **2004**, *60*, 344–345.
- Rodriguez-Cuamatzi, P.; Vargas-Diaz, G.; Maris, T.; Wuest, J. D.; Höpfl, H. *Acta Crystallogr. E* **2004**, *60*, 1316–1318.
- Rettig, S. J.; Trotter, J. *Can. J. Chem.* **1977**, *55*, 3071–3075.
- Vargas, R.; Garza, J.; Friesner, R. A.; Stern, H.; Hay, B. P.; Dixon, D. A. *J. Phys. Chem. A* **2001**, *105*, 4963–4968.
- Besley, N. A.; Hirst, J. D. *J. Am. Chem. Soc.* **1999**, *121*, 8559–8566.
- Desfrancois, C.; Périquet, V.; Carles, S.; Schermann, J. P.; Adamowicz, L. *Chem. Phys.* **1998**, *239*, 475–483.
- Gilli, G.; Gilli, P. *J. Mol. Struct.* **2000**, *552*, 1–15.
- Gora, R. W.; Grabowski, S. J.; Leszczynski, J. *J. Phys. Chem. A* **2005**, *109*, 6397–6405.
- Dabrowski, M.; Lulinski, S.; Serwatowski, J.; Szczerbinska, M. *Acta Crystallogr.* **2006**, *62*, 702–704.
- Saygili, N.; Batsanov, A. S.; Bryce, M. R. *Org. Biomol. Chem.* **2004**, *2* (6), 852–857.
- McKee, M. L. *J. Phys. Chem.* **1996**, *100*, 8260–8267.
- Møller, C.; Plesset, M. S. *Pure Appl. Chem.* **1934**, *46*, 618–622.
- Cizek, J. *Adv. Chem. Phys.* **1969**, *14*, 35–89.
- Purvis, G. D., III; Bartlett, R. J. *J. Chem. Phys.* **1982**, *76*, 1910–1918.
- Scuseria, G. E.; Janssen, C. L.; Schaefer, H. F. *J. Chem. Phys.* **1988**, *89*, 7382–7387.
- Scuseria, G. E.; Schaefer, H. F. *J. Chem. Phys.* **1989**, *90*, 3700–3703.
- Krishnan, R.; Binkley, J. S.; Seeger, R.; Pople, J. A. *J. Chem. Phys.* **1980**, *72*, 650–654.
- Clark, T.; Chandrasekhar, J.; Spitznagel, G. W.; Von Ragué Schleyer, P. *J. Comput. Chem.* **2004**, *4*, 294–301.
- Dunning, T. H. *J. Chem. Phys.* **1989**, *90*, 1007–1023.

- (62) Woon, D. E.; Dunning, T. H. *J. Chem. Phys.* **1993**, *98*, 1358–1371.
- (63) Kendall, R. A.; Dunning, T. H., Jr. *J. Chem. Phys.* **1992**, *96*, 6796–6806.
- (64) Peterson, K. A.; Woon, D. E.; Dunning, T. H., Jr. *J. Chem. Phys.* **1994**, *100*, 7410–7415.
- (65) Larkin, J. D.; Bhat, K. L.; Markham, G. D.; Brooks, B. R.; Schaefer, H. F., III; Bock, C. W. *J. Phys. Chem. A* **2006**, *110*, 10633–10642.
- (66) Dembitsky, V. M.; Quntar, A. A.; Srebnik, M. *Mini Rev. Med. Chem.* **2004**, *4*, 1001–1018.
- (67) Lindquist, R.; Nguyen, A. *J. Am. Chem. Soc.* **1977**, *99* (19), 6435–6437.
- (68) Amssoms, K.; Oza, S.; Ravaschino, E.; Yamani, A.; Lambeir, A.; Rajan, P.; Bal, G.; Rodriguez, J.; Fairlamb, A.; Augustyns, K.; Haemers, A. *Bioorg. Med. Chem. Lett.* **2002**, *12* (18), 2553–2556.
- (69) Matteson, D. S. *Stereodirected Synthesis with Organoboranes*; Springer: Berlin, 1995; pp 120–161.
- (70) Rogowska, P.; Cyranski, M.; Sporzynski, A.; Ciesielski, A. *Tetradedron Letts.* **2006**, *47*, 1387–1393.
- (71) James, T. D.; Sandanayake, K. R. A. S.; Shinkai, S. *Angew. Chem., Int. Ed. Engl.* **1996**, *35*, 1910–1922.
- (72) James, T. D.; Shinkai, S. *Top. Curr. Chem.* **2002**, *218*, 159–164.
- (73) Mohler, L. K.; Czarnik, A. W. *J. Am. Chem. Soc.* **1993**, *115*, 7037–7038.
- (74) Bhat, K. L.; Howard, N. J.; Rostami, H.; Lai, J. H.; Bock, C. W. *J. Mol. Struct. (THEOCHEM)* **2005**, *723*, 147–157.
- (75) Reinhardt, S.; Marian, C. M.; Priv.-Doz; Irmgard, F. *Angew. Chem., Int. Ed. Engl.* **2001**, *40*, 3683–3685.
- (76) Lynch, B. J.; Fast, P. L.; Harris, M.; Truhlar, D. G. *J. Phys. Chem. A* **2000**, *104*, 4811–4815.
- (77) Tsuzuki, S.; Lüthi, H. P. *J. Chem. Phys.* **2001**, *114*, 3949–3957.
- (78) Ahlrichs, R.; Furche, F.; Grimme, S. *Chem. Phys. Lett.* **2000**, *325*, 317–321.
- (79) Holme, T. A.; Truong, T. N. *Chem. Phys. Lett.* **1993**, *215*, 53–57.
- (80) Frisch, M. J.; Trucks, G. W.; Schlegel, H. B.; Scuseria, G. E.; Robb, M. A.; Cheeseman, J. R.; Montgomery, J. A., Jr.; Vreven, T.; Kudin, K. N.; Burant, J. C.; Millam, J. M.; Iyengar, S. S.; Tomasi, J.; Barone, V.; Mennucci, B.; Cossi, M.; Scalmani, G.; Rega, N.; Petersson, G. A.; Nakatsuji, H.; Hada, M.; Ehara, M.; Toyota, K.; Fukuda, R.; Hasegawa, J.; Ishida, M.; Naskajima, T.; Honda, Y.; Kitao, O.; Nakai, H.; Klene, M.; Li, X.; Knox, J. E.; Hratchian, H. P.; Cross, J. B.; Adamo, C.; Jaramillo, J.; Gomperts, R.; Stratmann, R. E.; Yazyev, O.; Austin, A. J.; Cammi, R.; Pomelli, C.; Ochterski, J. W.; Ayala, P. Y.; Morokuma, K.; Voth, G. A.; Salvador, P.; Dannenberg, J. J.; Zakrzewski, V. G.; Dapprich, S.; Daniels, A. D.; Strain, M. C.; Farkas, O.; Malick, D. K.; Rabuck, A. D.; Raghavachari, K.; Foresman, J. B.; Ortiz, J. V.; Cui, Q.; Baboul, A. G.; Clifford, S.; Cioslowski, J.; Stefanov, B. B.; Liu, G.; Liashenko, A.; Piskorz, P.; Komaromi, I.; Martin, R. L.; Fox, D. J.; Keith, T.; Al-Laham, M. A.; Peng, C. Y.; Nanayakkara, A.; Challacombe, M.; Gill, P. M. G.; Johnson, B.; Chen, W.; Wong, M. W.; Gonzalez, C.; Pople, J. A. *Gaussian03*, revision B.02; Gaussian Inc.: Wallingford, CT, 2003.
- (81) Carpenter, J. E.; Weinhold, F. *J. Mol. Struct. (THEOCHEM)* **1988**, *169*, 41–62.
- (82) Curtiss, L. A.; Weinhold, F. *Chem. Rev.* **1988**, *88*, 899–926.
- (83) Foster, J. P.; Weinhold, F. *J. Am. Chem. Soc.* **1980**, *102*, 7211–7218.
- (84) Reed, A. E.; Weinhold, F. *J. Chem. Phys.* **1983**, *78* (6), 4066–4073.
- (85) Reed, A. E.; Weinstock, R. B.; Weinhold, F. *J. Chem. Phys.* **1985**, *83* (2), 735–746.
- (86) Lee, C.; Yang, W.; Parr, R. G. *Phys. Rev. B. Condens. Matter* **1988**, *37* (2), 785–789.
- (87) Becke, A. D. *J. Chem. Phys.* **1993**, *98* (7), 5648–5652.
- (88) Handy, N. C.; Cohen, A. J. *Mol. Phys.* **2001**, *99*, 403–412.
- (89) Cohen, A. J.; Handy, N. C. *Mol. Phys.* **2001**, *99*, 607–615.
- (90) Perdew, J. P.; Burke, K.; Ernzerhof, M. *Phys. Rev. Lett.* **1997**, *78* (7), 1396–1396.
- (91) Rabuck, A. D.; Scuseria, G. E. *Chem. Phys. Lett.* **1999**, *309*, 450–456.
- (92) Perdew, J. P.; Burke, K.; Ernzerhof, M. *Phys. Rev. Lett.* **1996**, *77*, 3865–3868.
- (93) Staroverov, V. N.; Scuseria, G. E.; Tao, J.; Perdew, J. P. *J. Chem. Phys.* **2003**, *119*, 12129–12137.
- (94) Cancès, E.; Mennucci, B.; Tomasi, J. *J. Chem. Phys.* **1997**, *107*, 3032–3041.
- (95) Mennucci, B.; Tomasi, J. *J. Chem. Phys.* **1997**, *106*, 5151–5158.
- (96) Mennucci, B.; Cancès, E.; Tomasi, J. *J. Phys. Chem. B* **1997**, *101*, 10506–10517.
- (97) Cossi, M.; Barone, V.; Mennucci, B.; Tomasi, J. *Chem. Phys. Lett.* **1998**, *286*, 253–260.
- (98) Cossi, M.; Scalmani, G.; Rega, N.; Barone, V. *J. Chem. Phys.* **2002**, *117*, 43–54.
- (99) Castejon, H.; Wiberg, K. B. *J. Am. Chem. Soc.* **1999**, *121*, 2139–2149.
- (100) Castejon, H.; Wiberg, K. B.; Sklenak, S.; Hinz, W. *J. Am. Chem. Soc.* **2001**, *123* (25), 6092–6097.
- (101) Andzelm, J.; Koelmel, C.; Klamt, A. *J. Chem. Phys.* **1995**, *103*, 9312–9320.
- (102) Baldrige, K.; Klamt, A. *J. Chem. Phys.* **1997**, *106*, 6622–6633.
- (103) Klamt, A.; Jonas, V. *J. Chem. Phys.* **1996**, *105*, 9972–9981.
- (104) Klamt, A.; Schüümann, G. *J. Chem. Soc., Perkin Trans.* **1993**, *2*, 799–805.
- (105) *PQS Ab Initio Program Package 3.2*; Parallel Quantum Solutions: Fayetteville, AR, 2005.
- (106) Klamt, A. *J. Phys. Chem.* **1995**, *99*, 2224–2235.
- (107) Klamt, A.; Jonas, V.; Bürger, T.; Lohrenz, J. C. W. *J. Phys. Chem. A* **1998**, *102*, 5074–5085.
- (108) Perdew, J. P. *Phys. Rev. B* **1986**, *33*, 8822–8824.
- (109) Perdew, J. P.; Zunger, A. *Phys. Rev. B* **1981**, *23*, 5048–5079.
- (110) Vosko, S. H.; Wilk, L.; Nusair, M. *Can. J. Phys.* **1980**, *58*, 1200–1211.
- (111) Schäfer, A.; Horn, H.; Ahlrichs, R. *J. Chem. Phys.* **1992**, *97*, 2571–2577.
- (112) Schäfer, A.; Huber, C.; Ahlrichs, R. *J. Chem. Phys.* **1994**, *100*, 5829–5835.
- (113) Lai, J. H. Personal Communication.
- (114) Laplante, C.; Hall, D. G. *Org. Lett.* **2001**, *3* (10), 1487–1490.
- (115) Larkin, J. D.; Bhat, K. L.; Markham, G. D.; Brooks, B. R.; Lai, J. H.; Bock, C. W. *J. Phys. Chem.*, in press.
- (116) Bhat, K. L.; Braz, V.; Laverty, E.; Bock, C. W. *J. Mol. Struct. (THEOCHEM)* **2004**, *712*, 9–19.
- (117) Bhat, K. L.; Hayik, S.; Corvo, J. N.; Marycz, D. M.; Bock, C. W. *J. Mol. Struct. (THEOCHEM)* **2004**, *673*, 145–154.
- (118) We also optimized the analogous structure of the CH₃–B(OH)₂ dimer, and the OH···O hydrogen bond length was only ~0.005 Å shorter than that found for the H–B(OH)₂ dimer at the same computational levels.
- (119) Bock, C. W. Unpublished results.
- (120) Geller, S. *J. Chem. Phys.* **1960**, *32*, 1569–1570.
- (121) Dvorak, M. A.; Ford, R. A.; Suenram, R. D.; Lovas, F. J.; Leopold, K. R. *J. Am. Chem. Soc.* **1992**, *114*, 108–115.
- (122) Höpfl, H. *J. Organomet. Chem.* **1999**, *581*, 129–149.
- (123) These SCRFP CM PBE1PBE/6-311++G(d,p) calculations often proved problematical: in some cases the calculations failed unless the additional spheres added to smooth the surface representing the solvent–solute boundary were removed; in other cases, the calculations converged to structures that were transition states with low imaginary frequencies (~10 cm⁻¹) and repeated attempts to locate the corresponding local minima were unsuccessful. Typically, conformers with one or two B:N dative bonds, e.g., **5a**, **5b**, **6**, and **9a**, were stable at this level, whereas conformers with one or two O–H···O hydrogen bonds but no B:N dative bond, e.g., **1**, **3**, and **7**, were transition states; the doubly oxygen-bridged conformers **2** and **8** were also transition states.
- (124) Tao, J.; Perdew, J. P.; Staroverov, V. N.; Scuseria, G. E. *Phys. Rev. Lett.* **2003**, *91*, 146401–146404.
- (125) Barder, T. E.; Walker, S. D.; Martinelli, J. R.; Buchwald, S. L. *J. Am. Chem. Soc.* **2005**, *127*, 4685–4696.